International Journal of Concrete Structures and Materials

RESEARCH

Open Access

Tensile and Fracture Properties of Silicon Carbide Whisker-Modified Cement-Based Materials

Tao Shi[1,2*], Yingjia Lan[1], Zhuojun Hu[1], Haobo Wang[1], Jinhao Xu[1] and Bingmiao Zheng[1]

Abstract

Silicon carbide whiskers (SiCw) have many excellent properties such as high strength, high elastic modulus, and high temperature resistance. In this paper, by using water reducer as dispersant, a stable SiCw dispersion was obtained, and SiCw-modified cement-based composites were prepared. Tensile strength tests for 8-shaped specimens were carried out on the materials. The fracture properties of the materials were measured using a three-point bending test with pre-cracks based on the digital image correlation method. The microstructure of the SiCw-modified mortar was observed by SEM. The results showed that the SiCw improved the tensile strength of the cement-based materials, and the addition of SiCw effectively improved the fracture toughness of mortar. The SiCw caused crack deflection during crack propagation, accompanied by whisker pull-out and bridging phenomena. The SiCw bridging effect and pull-out mechanism effectively controlled the crack propagation and played a toughening role, thus enhancing the crack resistance of mortar.

Keywords: silicon carbide whiskers, cement-based materials, tensile strength, fracture toughness, microstructure

1 Introduction

Silicon carbide whiskers (SiCw) are a kind of material with high strength, a high elastic modulus, high temperature resistance, and good corrosion resistance (Becher et al., 2005; Peng et al., 2012). They are mostly used to modify ceramic-based (Silvestroni et al., 2010; Zhang et al., 2008) and metal-based (Zhang et al., 2006) materials, but have seldom been used in cement-based materials. Previous studies showing that the improvement of compressive strength with the addition of SiCw was not as great as that observed for the flexural strength, and hydration of the cement was accelerated by SiCw due to the higher number of nucleation sites, which results in a greater amount of nucleus formation (de Azevedo & Gleize, 2018; de Azevedo et al., 2021). Li studies demonstrated that the SiCw has a minor effect on the compressive strength of oil-well cement, but has great effect on the flexibility, spilt tensile strength and microstructure of oil-well cement (Li et al., 2019).

Cement-based materials are quasi-brittle materials, and their compressive strength is higher than their tensile strength (Bentur & Mindess, 2006). For such materials, a common shortcoming is brittle cracking. To solve this problem, there have been many studies on modifying cement-based materials, such as adding various organic materials or inorganic fibers (i.e., carbon nanomaterials or whiskers). (Chandrasekaran & Ramakrishna, 2021; Saulat et al., 2020; Shi et al., 2019; Yang et al., 2021; Zhan et al., 2020; Zhou et al., 2021). Whiskers are micro- and nano-sized short fibers grown from single crystals. Calcium carbonate whiskers (Cao et al., 2016; Saulat et al., 2020) and calcium sulfate whiskers (Li et al., 2017; Pan et al., 2019) are common whiskers used to improve the mechanical properties of cement-based materials.

*Correspondence: shitao@zjut.edu.cn
[1] College of Civil Engineering, Zhejiang University of Technology, Hangzhou 310023, China
Full list of author information is available at the end of the article
Journal information: ISSN 1976-0485 / eISSN 2234-1315

However, the strength and hardness of these whiskers are far lower than those of SiCw. Combining SiCw and cement-based materials to construct a new material system is a new idea for solving the brittleness problem in cement-based materials.

Herein, the preparation of an SiCw dispersion was explored. A stable and homogeneous SiCw dispersion was prepared and added to cement mortar. Mechanical property tests on cement mortar containing different dosages of SiCw were carried out to determine the influence of SiCw addition on the tensile and fracture properties of cement-based materials. The strengthening mechanism was analyzed based on scanning electron microscopy (SEM) imaging.

Fig. 1 SEM image of the SiCw.

2 Materials and Methods

2.1 Materials

2.1.1 SiCw

The SiCw used in this test were produced by Beijing Huawei Ruike Chemical Co., Ltd. The properties of the whiskers are shown in Table 1.

The whiskers were observed using scanning electron microscopy, and their microscopic morphology is shown in Fig. 1. The X-ray diffraction (XRD) pattern of the whiskers is shown in Fig. 2.

2.1.2 Cement and Other Materials

P·II52.5 grade Portland cement was used in this experiment, and the chemical composition of the cement is listed in Table 2. The fine aggregate used in the experiment was China ISO standard sand according to ISO679 and EN196-1 specifications manufactured by Xiamen ISO Standard Sand Co., Ltd.

The needle-like shape of the SiCw leads to poor fluidity (Lv et al., 2019), and the specific surface area of SiCw is large. Thus, there is a large van der Waals force between the whiskers, which makes it difficult to disperse the SiCw. The ZWL-PC series polycarboxylate superplasticizer produced by Zhejiang Wulong New Material Co., Ltd. was selected as the dispersant for the SiCw. Moreover, in order to better disperse the SiCw in the cement-based materials, in addition to adding the dispersant, the pH value of the dispersion solution was adjusted to optimize the dispersion (Xiong et al., 2008). In this experiment, calcium hydroxide was used to adjust the pH.

Table 1 Properties of the SiCw.

Crystal type	Beta
Average diameter	600 nm
Length	10–20 μm
Specific surface area	30 m^2/g
Particle morphology	Fibrous
Color	Greyish-green
Density (15 °C)	3.216 g/cm^3
Bulk density	0.74 g/cm^3
Hardness (Mohs)	9.5
Compressibility	0.21×10^{-6}

2.2 Methods

2.2.1 Preparation of the SiCw Dispersion

The SiCw dispersion was composed of SiCw, deionized water, dispersant, and pH regulator. The effectiveness of the dispersion was related to various factors such as the magnetic stirring time, ultrasonic dispersion time, pH

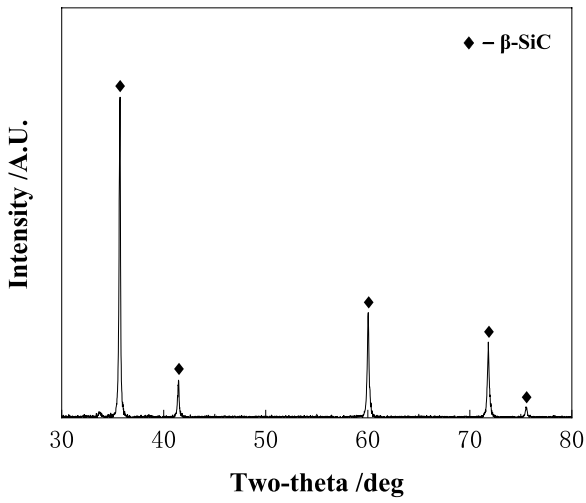

Fig. 2 XRD pattern of the SiCw.

Table 2 Chemical compositions of the cement/wt%.

Material	CaO	SiO_2	Al_2O_3	Fe_2O_3	SO_3	MgO	Loss
Cement	64.47	22.18	4.51	3.15	2.56	1.2	1.36

Table 3 Factors and levels used in the orthogonal experimental design.

Factor level	Factor			
	Dosage of water reducer (%) A	Magnetic stirring time (min) B	Ultrasonic dispersion time (min) C	pH D
1	0.3	5	1	7
2	0.4	10	2	9
3	0.5	15	4	11

value of solution, and dosage of the water reducing agent (Zhao et al., 2018). Considering there are many influencing factors, an orthogonal test with four factors and three levels was designed to optimize the SiCw dispersion (Kang et al., 2021), and the factors and their levels are shown in Table 3.

The L_9 (3^4) orthogonal table is shown in Table 5 (in Sect. 3.1). The dispersion rate of the SiCw measured by the relative settlement method was used as the index to perform the quantitative analysis of the results of the nine test groups. Based on the analysis results, the optimal dispersion scheme and the influence of the various factors on the dispersion (the primary and secondary subsequences) were determined.

The dispersion rate of the SiCw was measured by the relative sedimentation method. In the relative sedimentation method, the SiCw dispersion was left to set for a scheduled time period, and then the stratification phenomenon was analyzed. The specific order of operations was as follows. For each group, the SiCw dosage was 0.4%. After dispersion, 40 mL of the SiCw dispersion was poured into a test tube immediately, and the initial dispersion height (H_0) was measured. After the solution was left standing for the scheduled time period, the dividing line height (H_l) (Ding et al., 2020) of each group was measured. Thus, H_l/H_0 was the dispersion rate and was taken as the test index. A higher dispersion rate corresponded to a better SiCw dispersion.

2.2.2 Homogeneous Stability Test of SiCw Dispersion

The homogeneous stability of the SiCw dispersion is the most important characteristic of dispersed materials. In this paper, the factors that have significant influences on the dispersion were taken as variables, and the Zeta potential method and turbidimetry method were used to characterize the homogeneous stability of the SiCw dispersions and were used to verify the accuracy of the orthogonal test results.

2.2.2.1 Zeta Potential Method The surface Zeta potential of the SiCw was measured by placing the SiCw dispersion in a Nano ZS90 Malvern nano-particle analyzer. According to the Stern double-layer structure principle (Greenwood, 2003), the greater the absolute value of the surface Zeta potential, the greater the repulsion force between the whiskers and the more difficult it is for the whiskers to agglomerate, corresponding to a more stable the dispersion (Mutsuddy, 1990).

2.2.2.2 Turbidimetry When ultraviolet light passes through a suspension, it is scattered or absorbed by the suspended particles, thus reducing the light transmittance (Wang et al., 2019). Based on this phenomenon, the measured absorbance can be used to compare the turbidity of the suspensions. In our experiment, the absorbance of the supernatant of the SiCw dispersion after standing for the specified time was measured using a UV spectrophotometer, and the measured absorbance reflected the amount of SiCw in the superliquid of the dispersed liquid after standing.

Generally, performing a full band scan with the UV spectrophotometer requires a long time. In order to improve the experimental efficiency, a full band scan of a SiCw dispersion was carried out with the UV spectrophotometer to determine the peak wavelength of the absorbance curve. As shown in Fig. 3, the peak wavelength was about 198 nm. Then, only a partial band scan over a wavelength range from 150 to 250 nm was carried out on the samples.

2.2.3 Preparation of the SiCw-Modified Cement Mortar

First, the SiCw dispersion was prepared. The SiCw dispersion was composed of SiCw, water, dispersant, and the pH regulator. The preparation process was as follows. According to the optimal scheme, calcium hydroxide (pH regulator) was added to water to change the pH value of the aqueous solution, and then the water reducer (dispersant) and SiCw were added to the solution. Afterwards, the suspension was subjected to magnetic stirring and ultrasonic treatment to obtain a stable dispersion. Second, the cement and well-graded sand were dry-blended

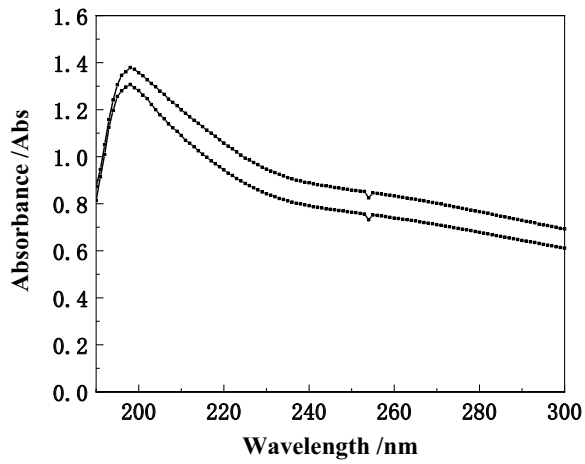

Fig. 3 SiCw dispersion scanned with a UV spectrophotometer.

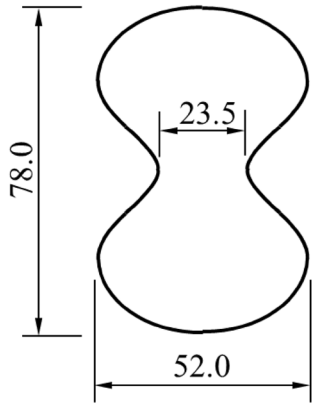

Fig. 4 8-shaped specimen size/mm.

Fig. 5 Tensile test device.

Table 4 Mix proportions of mortar with different dosages of SiCw.

Specimen group	SiCw/wt%	Water reducer/wt%	CH solution	Cement	Sand
SiC-0	0	0.15	0.5	1	3
SiC-0.1	0.1				
SiC-0.2	0.2				
SiC-0.3	0.3				

to a homogeneous state, and then the prepared dispersion was added to the homogeneous mixture. The mixture was blended evenly using a glue sand mixer and then poured into a mold. After 24 h, the mold was removed, and the specimens were put into a curing room at a temperature of 20 ± 2 °C with a humidity of 95% for different ages (7, 14 and 28 days). The specific mix proportions for preparing the cement mortar are shown in Table 4.

2.2.4 Tensile Tests for 8-shaped Specimens

Fig. 4 shows a schematic of the 8-shaped mortar specimens (with a thickness of 22.2 mm) designed for this experiment. The 8-shaped specimens are easier to use during the tensile test, and the measured tensile data are less discrete and are more reliable (Ou, 2012). Considering the middle cross-sectional area of 8-shaped specimens is small, theoretically, the specimens should fracture in the middle during the loading process. In the pre-test, it was confirmed that the 8-shaped specimens had a consistent fracture positions, i.e., in the middle of the specimens, when they fractured.

Tensile tests were conducted on the cement-based composites with different SiCw dosages (ASTM C307-18, 2018; Meng et al., 2019). A WDW-50KN testing machine, as shown in Fig. 5, was used for the displacement loading with a loading rate of 1 mm/min. In order to avoid the influence of the relative slip between the fixture and the specimens on the displacement measurement at the initial stage of loading, preloaded to the load of 100 kN, zeroed the displacement, and then continued to load until the specimens were broken. For each group, the arithmetic mean of the measured values of five specimens was taken as the tensile strength value of the group.

2.2.5 Three-Point Bending Beam Test Based on the DIC Method

The dimensions of the specimens were 40 mm × 40 mm × 200 mm. As shown in Fig. 6, the width of the midspan pre-crack was 1 mm, and the spacing between supports was 160 mm.

The Digital Image Correlation (DIC) method was used to obtain the relevant parameters during the fracture process (Baietti et al., 2020; Zhang et al.,

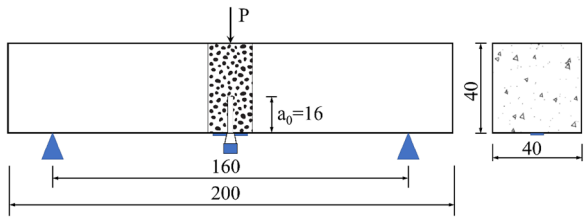

Fig. 6 Schematic diagram of specimen (mm).

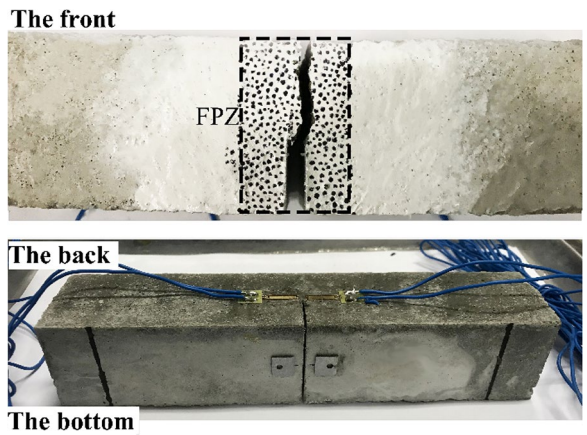

Fig. 7 Surface treatment of the specimens.

2018). The surface of the test specimens needed to be pretreated. As shown in Fig. 7, in order to obtain the digital speckle images required for DIC, a speckle pretreatment was performed on an area 20 mm × 40 mm in size in the fracture process zone (FPZ) on the front surface of the specimens (Yao et al., 2020). To obtain the initial crack load of the specimens, resistance strain gauges were pasted on the reverse surface of the specimen, and the pasted position was as close as possible to both sides of the crack tip. To measure the crack mouth opening displacement (CMOD) of the test specimens, steel sheets were affixed to both sides of the pre-crack at the bottom of the specimen to attach a YC10/2 clip-type extensometer. The clip-type extensometer and resistance gauges were connected with a TDS303 static strain data acquisition instrument to obtain the relevant data. There were four specimens in each group in order to ensure that each group obtained at least three valid data.

A WDW-50KN testing machine was used for the displacement loading, and the loading rate was 0.1 mm/min. The FPZ was imaged using a high-speed camera at a rate of 10 fps. In the test process, a strong light source was required to ensure clear images were captured of the specimens. The captured speckle images were pretreated by grey processing and then analyzed with MATLAB software (Kumar et al., 2019).

3 Results and Discussion

3.1 Optimal Preparation Scheme of the SiCw Dispersion

Table 5 gives the analysis results of the orthogonal experiment designed to determine the influencing factors of the SiCw dispersion.

In Table 5, K_i value represents the sum of test index values corresponding to the i level of a factor, and $k_i = K_i/3$. According to the characteristics of orthogonal design, an example is as follows: if factor A has no effect on the test index, k_1, k_2 and k_3 corresponding to A should be equal. If not, the optimal level of factor A can be obtained by comparing the sizes of k_1, k_2 and k_3. The optimal level combination of each factor can obtain an optimal combination.

R represents the range of a factor, which is calculated as follows: $R = \max(k_i) - \min(k_i)$ reflects the variation range of the test index when the factor fluctuates. The greater the R corresponding to the factor, the greater the impact of the factor on the test index. By comparing the range, R, the influences of the various factors on the dispersion of SiCw were determined as follows: pH value of solution > water reducer dosage > magnetic stirring time > ultrasonic dispersion time. According to the experimental results, a solution pH value of 11 and a water reducer dosage of 0.3% was the most conducive for dispersing the SiCw. After the addition of SiCw, the optimal treatment method was magnetic stirring for 15 min and then subsequent ultrasonic stirring for 4 min.

3.2 Influences of Solution pH Value and Water Reducer Dosage on the SiCw Dispersion

In order to further verify the accuracy of the orthogonal test results, the two most important factors affecting the effectiveness of the dispersion, i.e., the solution pH value and water reducer dosage, were tested by a single control variable experiment. The influences of the solution pH value and water reducer on the dispersion of SiCw were studied.

According to the results in Sect. 3.1, the solution pH value had the greatest influence on the dispersion of the whiskers. Fig. 8 shows the absorbance and Zeta potential of SiCw dispersions prepared in solutions with different pH values.

When the pH value of the solution was 11, the absolute value of the Zeta potential on the surface of the SiCw was the largest. According to Stern double electric layer structure principle (Greenwood, 2003), when the solution pH value was 11, the repulsive force between the SiCw was large, and it was not easy for the whiskers to agglomerate, thus producing the best dispersion effect of the SiCw. This result was consistent with the absorbance

Table 5 Analysis of the orthogonal experiments.

Parameter group number	Factor				Dispersion rate (%)
	Dosage of water reducer (%) A	Magnetic stirring time (min) B	Ultrasonic dispersion time (min) C	pH D	
1	0.3	5	1	7	78.1
2	0.3	10	2	9	82.7
3	0.3	15	4	11	89.7
4	0.4	5	2	11	80.6
5	0.4	10	4	7	77.5
6	0.4	15	1	9	77.4
7	0.5	5	4	9	77.7
8	0.5	10	1	11	84.5
9	0.5	15	2	7	81.3
K_1	250.5	236.4	240	236.9	
K_2	235.5	244.7	244.6	237.8	
K_3	243.5	248.4	244.9	254.8	
k_1	83.50	78.80	80.00	78.97	
k_2	78.50	81.57	81.53	79.27	
k_3	81.17	82.80	81.63	84.93	
R	5	4	1.63	5.97	
The primary and secondary subsequence	$D>A>B>C$				
Optimal level	A_1	B_3	C_3	D_3	
Optimal condition	$A_1B_3C_3D_3$				

The dosage of SiCw in each group is 0.4%.

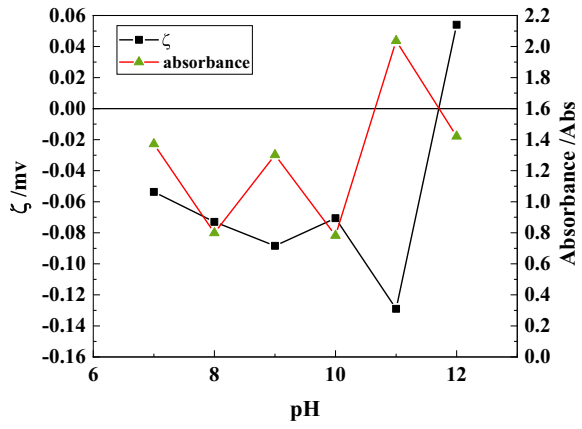

Fig. 8 Zeta potential and absorbance of SiCw as a function of pH.

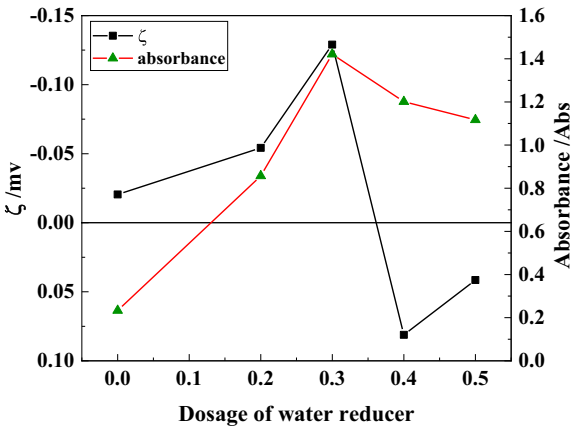

Fig.9 Zeta potential and absorbance of SiCw as a function of the water reducer dosage.

results. When the pH value was 11, the absorbance was the highest because the superliquid of the SiCw dispersion prepared in a solution with a pH value of 11 had the highest whisker dosage which scattered or absorbed more UV light and led to low light transmission and a high UV absorbance value. In other words, after standing, it was more difficult for the SiCw dispersion prepared in a pH 11 solution to stratify and precipitate.

The influence of the water reducer dosage on the dispersion of SiCw is second only to the solution pH value. Similarly, we took the water reducer dosage as the variable to determine the absorbance and Zeta potential, and the results are shown in Fig. 9. As can be seen, the dispersion effect is the best when the dosage of the water reducer was 0.3%.

3.3 Influence of SiCw Addition on the Tensile Properties of Cement Mortar

Fig. 10 shows the tensile strength of the cement mortar at different curing ages. The addition of SiCw improved the tensile strength of the cement mortar, the content of SiC whiskers with the content of 0.1%, 0.2% and 0.3% increased by 8.1%, 4.5% and 2.2%, respectively, at 28 days. There was an optimal SiCw dosage. The overall tensile performance of the cement mortar was best with a SiCw dosage of 0.1%. With an increase in the whisker dosage, the tensile performance of the cement mortar was not enhanced significantly. The reasons are summarized as follows. When the whisker dosage was low, the whiskers were dispersed evenly, and the toughening effect was significant (Wang et al., 2008; Zhu et al., 2021). As the SiCw dosage increased, the original defects in the material and the agglomeration entanglement of the SiCw had adverse effects on the tensile strength of mortar (Hambach et al., 2016). When the whisker dosage reached 0.3%, on the contrary, the tensile strength decreased significantly at 7 days, which may have been because the hydration products only wrapped the surface of the aggregates at an early age, but did not fill the gaps between the whiskers (Bentur & Mindess, 2006; Cuixiang et al., 2011).

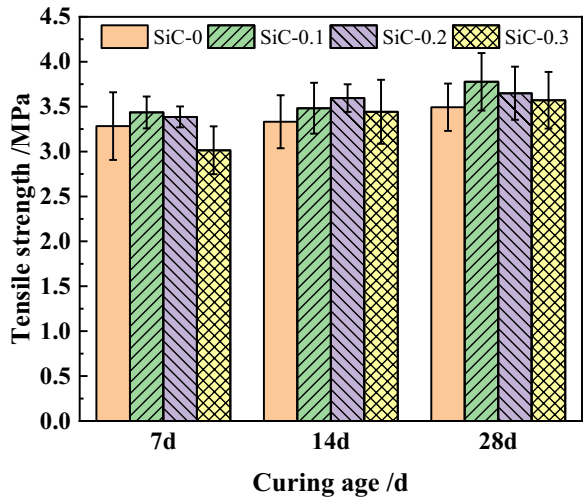

Fig.10 Tensile strength of mortars with different SiCw dosages.

From tensile tests of the 8-shaped mortars, the stress–displacement curves for different whisker dosages were obtained, and the results are shown in Fig. 11. For the blank group, with an increase in the curing age, the displacement of the stress peak increased first and then decreased. For the 7-day specimen group, the mortar strength was still very low, and the specimens broke easily. For the 14-day specimen group, further hydration of the cement enhanced the mortar strength to some extent, and the tensile strength also improved, so the displacement corresponding to stress peak value increased. After 28 days, the strength of mortar was further enhanced, and the mortar was significantly more brittle, so the displacement corresponding to the stress peak value decreased slightly.

The addition of SiCw delayed the specimens from reaching their peak stress value and increased their tensile strength to a certain extent. It can be seen that the tensile strengths of the test groups with dosages of 0.1% and 0.2% both improved to a certain extent, of which, the tensile performance for the specimen with a SiCw dosage of 0.1% was slightly better than that with 0.2%. However, due to the progress of the cement hydration, the mortar became more and more brittle, and the displacement corresponding to the peak stress value also gradually decreased. For the test group with an SiCw dosage of 0.3%, the strength deteriorated, and the peak displacement increased significantly. This may have been due to the high dosage of SiCw in the cement matrix leading to the formation of agglomerates and entanglements (Ren et al., 2013).

The work done during the tensile test was obtained by integrating the stress–displacement curves, as shown in

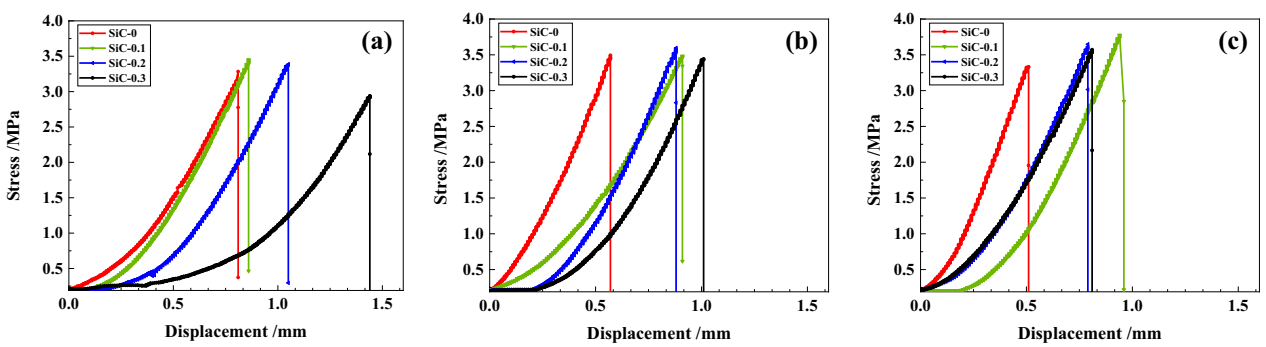

Fig. 11 Stress–displacement curves of cement mortar modified by SiCw at different age: **a** 7 days, **b** 14 days, **c** 28 days.

Fig. 12. The experimental results showed that the addition of SiCw increased the energy consumption during the tensile process and effectively played a role in toughening the cement-based materials. For the 28-day specimens, the energy consumption of the experimental group with the SiCw dosage of 0.1% was 67.9% higher than that of the blank group.

At an age of 7 days, for SiCw dosages of 0.2% and 0.3%, the whisker entanglement caused by the higher SiCw dosage significantly contributed to the energy consumption during the tensile tests at the initial stages of cement hydration. In contrast, for the SiCw dosage of 0.1%, at the initial stage of cement hydration, the whisker dispersion was relatively homogeneous, but the insufficient cement hydration led to a weak holding force on the whiskers. As a result, the whiskers were pulled out easily rather than breaking, and their energy consumption was not obvious.

At 14 days of aging, for the SiCw dosages of 0.2% and 0.3%, the adverse effects of cement hardening on the toughness were much higher than the improvements from the inhomogeneous dispersion of the whiskers. For the SiCw dosage of 0.1%, with further cement hydration, the hydration products filled the gaps between the whiskers, and the whiskers were wrapped by the cement matrix, significantly enhancing the toughness.

3.4 Influence of SiCw Addition on the Fracture Properties of Cement Mortar

Table 6 shows the results of the three-point bending tests on the specimens. The addition of the SiCw effectively increased the initial cracking load (P_{ini}) of the material and delayed cracking of the crack tip. The P_{ini} value of the specimen with 0.1% SiCw dosage was 9.8% higher than that of the blank group, and the deformation of the specimen with 0.1% SiCw dosage before the crack tip cracked was much higher than that of the blank group (Fig. 13). It can also be seen from the CMOD of the group with 0.1% SiCw content increased by 78.7%. Obviously, the brittleness of the cement mortar modified with the SiCw decreased. The maximum load (P_{max}) at fracture did not significantly increase. The specimen with 0.1% SiCw was only 6.1% higher than that of the blank group, but the unstable fracture toughness (K_{IC}^{un}) and CMOD were significantly enhanced, compared with the blank group, the group with 0.1% SiCw increased by 31.88% and 78.7%, respectively, which indicating that the addition of SiCw had an obvious effect on increasing the fracture

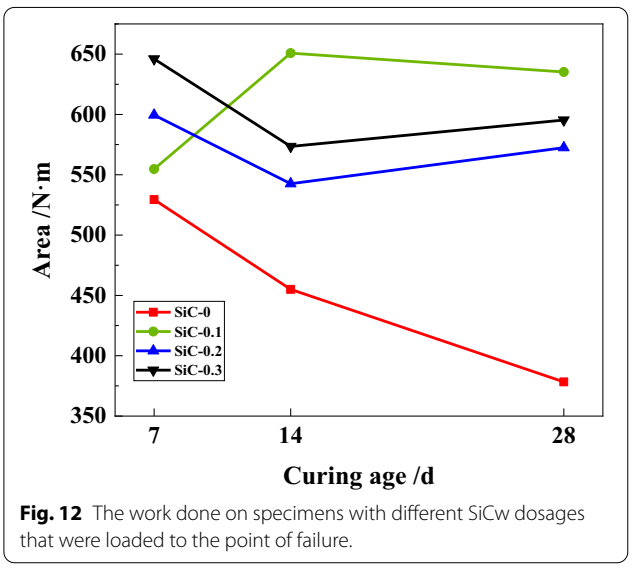

Fig. 12 The work done on specimens with different SiCw dosages that were loaded to the point of failure.

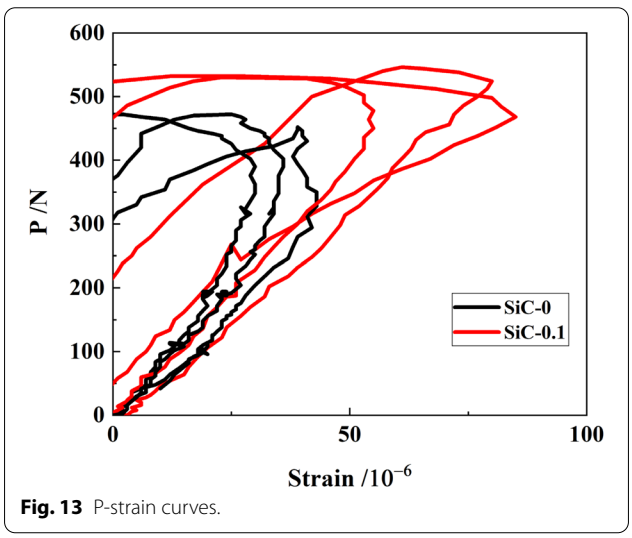

Fig. 13 P-strain curves.

Table 6 Three-point bending beam test results for cement mortars modified with SiCw.

Group	*E*/GPa	P_{ini}/kN	P_{max}/kN	CMOD/μm	a_c/mm	K_{IC}^{ini}/MPa · m$^{1/2}$	K_{IC}^{un}/MPa · m$^{1/2}$
SiCw-0	8.23	0.41(0.12)	0.49(0.03)	25.87(3.25)	20.75	0.11	0.69
SiCw-0.1	7.15	0.45(0.10)	0.52(0.01)	46.23(1.91)	22.69	0.12	0.91
SiCw-0.2	7.67	0.42(0.07)	0.50(0.03)	31.50(3.06)	21.52	0.12	0.75
SiCw-0.3	8.57	0.45(0.06)	0.51(0.03)	27.00(1.82)	21.05	0.12	0.74

The data are arithmetic mean of each group, and corresponding standard deviation is in brackets.

toughness of the cement mortar. Among the different addition dosages of SiCw, the toughening effect was the best when the SiCw dosage was 0.1%.

The P-CMOD curves of all test groups are shown in Fig. 14. When the whisker dosage was 0.1%, the discreteness of the P_{max} values decreased significantly, which may have been due to the whiskers being evenly dispersed, and their filling effect improved the initial defects in the cement-based materials. With an increase in the whisker dosage, the discreteness of the P_{max} values also increased. When the whisker dosage reached 0.3%, the P_{max} value decreased, indicating that too high of a whisker dosage led to an inhomogeneous SiCW dispersion, which affected the strength of the material. The addition of SiCw improved the CMOD, and the specimens achieved an increased maximum deformation during failure, indicating that the whiskers improved the brittleness of the cement-based materials and thus consumed more energy during the fracture process.

In order to further study the fracture process of the specimens, the displacement and strain cloud of the FPZ measured during the DIC treatment are provided in Fig. 15. Since the mechanical properties of the SiCw and cement-based materials were different, and SiCw have bridging, deflection, and pull-out effects on the cement-based materials (Becher et al., 2005), the stress state of the cement-based materials tended to be more complicated after the addition of the SiCw. It can be seen from Fig. 15 that, compared with the blank group, the specimens with added whiskers had more complex crack propagation paths and consumed more energy during the fracture process.

The images from left to right correspond to $P=0.6P_{max}$, $P=0.9P_{max}$, $P=P_{max}$, $P=0.8P_{max}$, and $P=0.2P_{max}$, respectively. As can be seen from the SiCw-0 group, at $P=0.9P_{max}$, even though the loading force was close to the maximum load that the specimen could bear, there was no obvious crack propagation at the tip of the pre-crack, but obvious cracks suddenly appeared at the tip of the pre-crack at $P=P_{max}$. However, after the addition of SiCw, there was an obvious toughening effect. Taking the SiCw-0.1 group with the best toughening effect as an example, the crack began to develop at $P=0.9P_{max}$, and the deformation was more obvious than that of the blank group. When the load reached $P=P_{max}$, although the

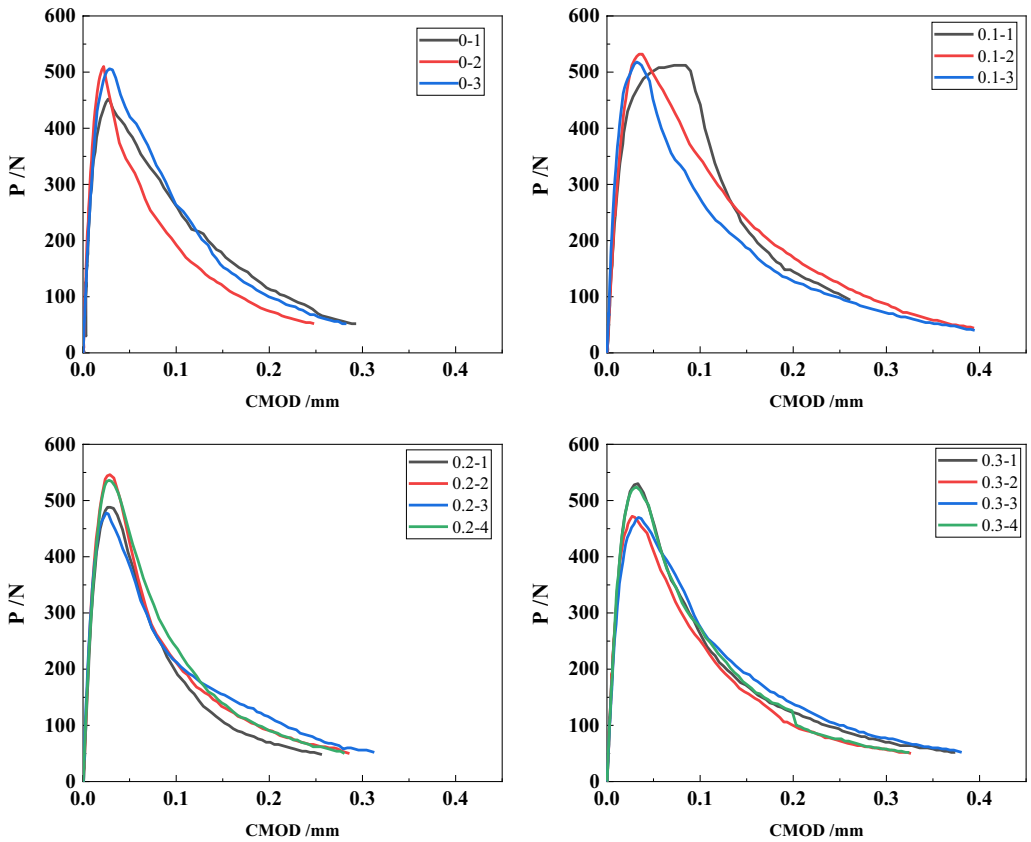

Fig. 14 P-CMOD curves (the label is in *x*–*y* form: "*x*" means the dosage of SiCw is *x*%, *y* is sample number).

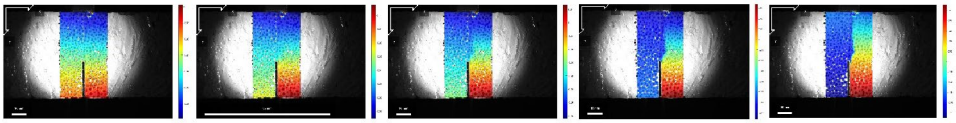

(a) Lateral displacement of FPZ: SiCw-0

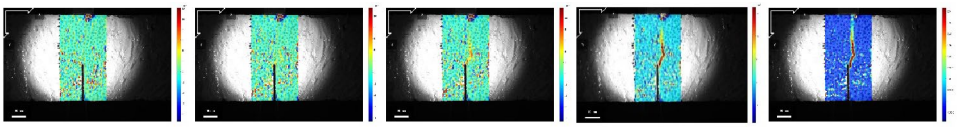

(b) Lateral strain of FPZ: SiCw-0

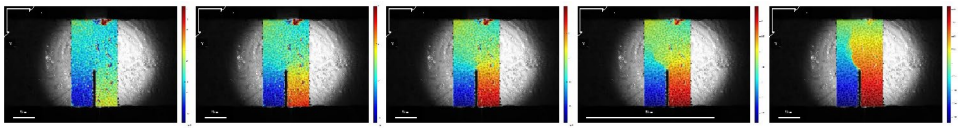

(c) Lateral displacement of FPZ: SiCw-0.1

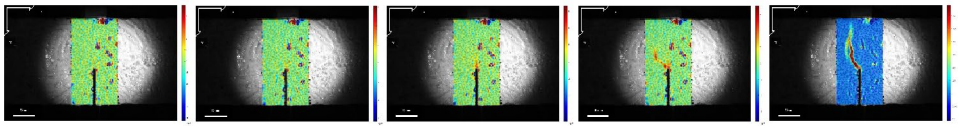

(d) Lateral strain of FPZ: SiCw-0.1

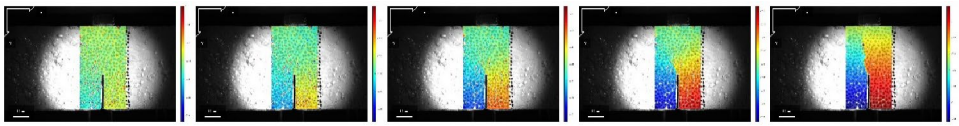

(e) Lateral displacement of FPZ: SiCw-0.2

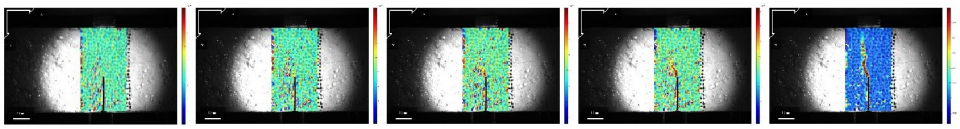

(f) Lateral strain of FPZ: SiCw-0.2

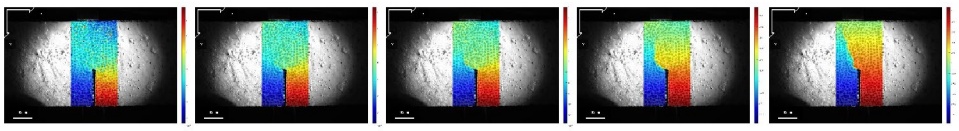

(g) Lateral displacement of FPZ: SiCw-0.3

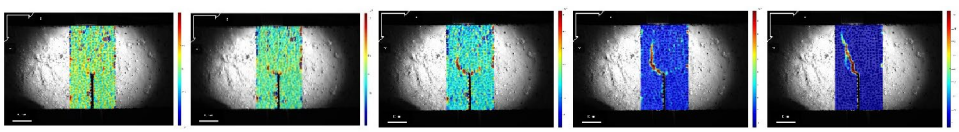

(h) Lateral strain of FPZ: SiCw-0.3

Fig. 15 Digital image processing results (from left to right are: $P=0.6P_{max}$, $P=0.9P_{max}$, $P=P_{max}$, $P=0.8P_{max}$, $P=0.2P_{max}$).

crack continued to develop, the crack length was far smaller than that of the blank group under the maximum load. As the loading process continued, the crack development in the blank group was basically stable at $P=0.8P_{max}$, but at this moment, the height of the unfractured zone of the specimen doped with SiCw was still very large, and the crack almost ran through the specimen until $P=0.2P_{max}$. These results indicated that the addition of SiCw obviously improved the brittleness of cement-based materials. Because cement-based materials are quasi-brittle materials, there was no significant deformation under stress, and fracture failure occurred suddenly once the stress surpassed the tensile strength. However, after the addition of SiCw, the deformation of the specimens under stress increased obviously. From the point of view of crack development, the cracks in the specimen modified by the SiCw developed slowly, and the failure was no longer sudden.

3.5 Microstructure Observation of Cement Mortar Modified by the SiCw

Fig. 16 shows the SEM results and EDS spectra measured at the crack in the SiCw-modified cement mortar. As can be seen, there were needle-like structures in the fractured positions of the specimens, which were confirmed to be SiCw by the EDS results.

The effectiveness of whiskers in enhancing the mechanical performance of mortar is dependent to a large extent on the whiskers–mortar interactions. There were bridging (Fig. 16a) and pull-out (Fig. 16b) phenomena from the SiCw in the fractured surface of the material. The pulled out SiCw surface was not bonded with a lot of cement matrix, the adhesional and frictional bonding between a SiC whisker and cementitious matrix may be relatively weak. They had however significant contribution and practical significance because of SiCw have a large surface area (Bentur & Mindess, 2006).When there was a shear stress at the interface between the cementitious matrix and SiCw, the crack deflected significantly,

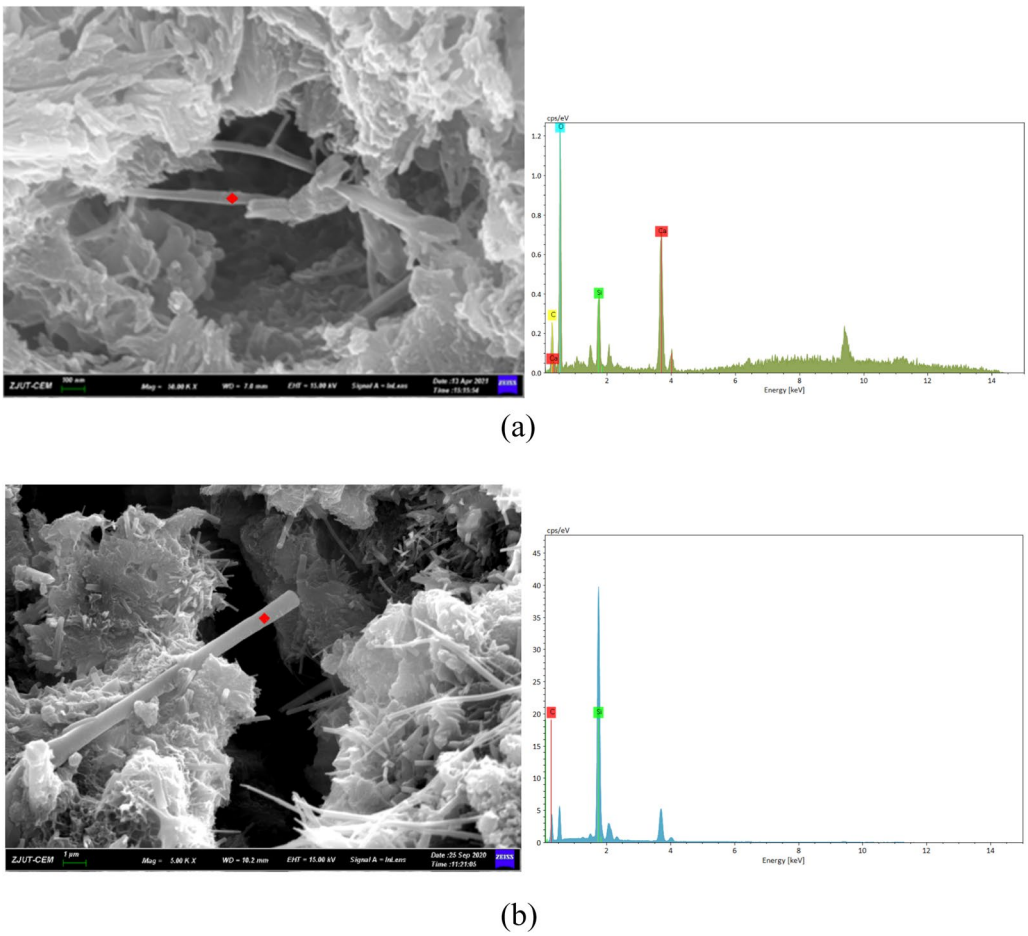

Fig. 16 SEM images of the morphology of the cement mortar modified by SiCw and EDS spectrum: **a** bridge effect, **b** pull-out.

and the whiskers fractured or pulled out of the matrix, thus consuming extra strain energy during the stress process. When the cement mortar was under tension, bridging of the whiskers effectively prevented the micro-crack propagation. This may have been the main mechanism of the SiCw reinforcement of the cement-based materials.

4 Conclusions

In summary, a new cement-based composite, i.e., a SiCw-modified cement-based composite, was prepared in this paper. The main conclusions are as follows:

(1) The solution pH and dispersant dosage were the main factors that affected the dispersion of the SiCw into an aqueous solution. When the solution pH value was about 11 and the dosage of water reducer was 0.3%, the dispersion of the SiCw was the best.
(2) The SiCw improved the tensile strength of the cement-based materials, and the optimal dosage was 0.1wt%.
(3) The fracture properties of the cement-based materials were effectively improved after the addition of SiCw. The values of P_{ini}, K_{IC}^{un}, and CMOD increased to a certain extent, which provided a new way to decrease the brittleness of cement-based materials.
(4) Based on the results from the microstructural observations and mechanical tests, it was speculated that the improvement in the tensile and fracture properties of cement-based composites by adding SiCw was due to the bridging effects of the SiCw, and the energy dissipation through the pull-out of the whiskers during crack propagation in the cement-based composites.

Acknowledgements
This work was supported by the National Natural Science Foundation of China [Grant Numbers 51778582, 52078460], the State Key Laboratory of Silicate Materials for Architectures (Wuhan University of Technology).

Authors' contributions
TS: conceptualization, methodology, supervision, writing—review and editing, funding acquisition. YL: visualization, data curation, writing—original draft preparation, software, methodology. ZH: project administration, resources. HW: supervision. JX: methodology, validation. BZ: software, methodology, validation. All authors read and approved the final manuscript.

Authors' information
Tao Shi, Professor in College of Civil Engineering, Zhejiang University of Technology, Hangzhou 310023, China, Key Laboratory of Civil Engineering Structures & Disaster Prevention and Mitigation Technology of Zhejiang Province, College of Civil Engineering, Zhejiang University of Technology, Hangzhou 310023, China. Yingjia Lan, Graduate student in College of Civil Engineering, Zhejiang University of Technology, Hangzhou 310023, China. Zhuojun Hu, Graduate student in College of Civil Engineering, Zhejiang University of Technology, Hangzhou 310023, China. Haobo Wang, Graduate student in College of Civil Engineering, Zhejiang University of Technology, Hangzhou 310023, China. Jinhao Xu, Graduate student in College of Civil Engineering, Zhejiang University of Technology, Hangzhou 310023, China. Bingmiao Zheng, Graduate student in College of Civil Engineering, Zhejiang University of Technology, Hangzhou 310023, China.

Funding
This work was supported by the National Natural Science Foundation of China [grant numbers 51778582, 52078460], the State Key Laboratory of Silicate Materials for Architectures (Wuhan University of Technology).

Availability of data and materials
The datasets used and/or analysed during the current study are available from the corresponding author on reasonable request.

Declarations

Competing interests
The authors declare that they have no known competing financial interests or personal relationships that could have appeared to influence the work reported in this paper.

Author details
[1]College of Civil Engineering, Zhejiang University of Technology, Hangzhou 310023, China. [2]Key Laboratory of Civil Engineering Structures & Disaster Prevention and Mitigation Technology of Zhejiang Province, College of Civil Engineering, Zhejiang University of Technology, Hangzhou 310023, China.

Received: 21 October 2021 Accepted: 17 December 2021
Published online: 01 February 2022

References

ASTM C307-18. (2018). *Standard test method for tensile strength of chemical-resistant mortar, grouts, and monolithic surfacings*. ASTM International.
Baietti, G., Quartarone, G., Carabba, L., Manzi, S., Carloni, C., & Bignozzi, M. C. (2020). Use of digital image analysis to determine fracture properties of alkali-activated mortars. *Engineering Fracture Mechanics, 240*, 107313.
Becher, P., Hsueh, C.-H., Angelini, P., & Tiegs, T. (2005). Toughening behavior in whisker-reinforced ceramic matrix composites. *Journal of the American Ceramic Society, 71*, 1050–1061.
Bentur, A., & Mindess, S. (2006). *Fibre reinforced cementitious composites*. CRC Press.
Cao, M., Xu, L., & Zhang, C. (2016). Rheology, fiber distribution and mechanical properties of calcium carbonate ($CaCO^3$) whisker reinforced cement mortar. *Composites Part A: Applied Science and Manufacturing, 90*, 662–669.
Chandrasekaran, R. G., & Ramakrishna, G. (2021). Experimental investigation on mechanical properties of economical local natural fibre reinforced cement mortar. *Materials Today: Proceedings*. https://doi.org/10.1016/j.matpr.2021.01.908
Cuixiang, J., Dongwang, Z., & Hao, h. (2011). Interface resistance between carbon fiber and cement. *Procedia Engineering, 15*, 5333–5337.
de Azevedo, N. H., de Matos, P. R., Gleize, P. J. P., & Betioli, A. M. (2021). Effect of thermal treatment of SiC nanowhiskers on rheological, hydration, mechanical and microstructure properties of Portland cement pastes. *Cement and Concrete Composites, 117*, 103903.
de Azevedo, N. H., & Gleize, P. J. P. (2018). Effect of silicon carbide nanowhiskers on hydration and mechanical properties of a Portland cement paste. *Construction and Building Materials, 169*, 388–395.
Ding, G., He, R., Zhang, K., Xia, M., Feng, C., & Fang, D. (2020). Dispersion and stability of SiC ceramic slurry for stereolithography. *Ceramics International, 46*(4), 4720–4729.
Greenwood, R. (2003). Review of the measurement of zeta potentials in concentrated aqueous suspensions using electroacoustics. *Advances in Colloid and Interface Science, 106*(1), 55–81.
Hambach, M., Möller, H., Neumann, T., & Volkmer, D. (2016). Portland cement paste with aligned carbon fibers exhibiting exceptionally high flexural strength (> 100MPa). *Cement and Concrete Research, 89*, 80–86.
Kang, P., Zhao, Q., Guo, S., Xue, W., Liu, H., Chao, Z., Jiang, L., & Wu, G. (2021). Optimisation of the spark plasma sintering process for high volume

fraction SiCp/Al composites by orthogonal experimental design. *Ceramics International, 47*(3), 3816–3825.
Kumar, S. L., Aravind, H. B., & Hossiney, N. (2019). Digital image correlation (DIC) for measuring strain in brick masonry specimen using Ncorr open source 2D MATLAB program. *Results in Engineering, 4*, 100061.
Li, M., Ye, K., Luo, K., Li, H., Su, Y., Li, G., & Mei, Y. (2017). Research progress on modification and applications in the material fields of calcium sulfate whisker. *Bulletin of the Chinese Ceramics Society, 36*(05), 1590-1593+1598.
Li, M., Yu, J., Zhang, C., Deng, S., Yu, Y., Yang, Y., & Guo, X. (2019). Hybrid effect, mechanical properties and enhancement mechanism of oil-well cement stone with multiscale silicon carbide whisker. *Journal of Adhesion Science and Technology, 33*(9), 903–920.
Lv, X., Ye, F., Cheng, L., Fan, S., & Liu, Y. (2019). Fabrication of SiC whisker-reinforced SiC ceramic matrix composites based on 3D printing and chemical vapor infiltration technology. *Journal of the European Ceramic Society, 39*(11), 3380–3386.
Meng, B., Xu, J., Liu, J., Gu, C., & Peng, G. (2019). Comparative experimental on effect of water content on tensile properties of cement mortar with two compounding ratios. *Bulletin of the Chinese Ceramics Society, 38*(1), 132–137.
Mutsuddy, B. (1990). Electrokinetic behavior of aqueous silicon carbide whisker suspensions. *Journal of the American Ceramic Society, 73*, 2747–2749.
Ou, Y., (2012). *Research of on-site detection technique for bond strength and compressive strength of ready-mixed mortar*. South China University of Technology
Pan, Q., Chen, T., Pan, R., Liu, B., & Li, D. (2019). Mechanical properties and microstructure of cementitious materials incorporated with calcium sulfate whiskers and silica fume. *Materials Reports, 33*(02), 257–263.
Peng, Y., Peng, Z., Ren, X., Rong, H., Wang, C., Fu, Z., Qi, L., & Miao, H. (2012). Effect of SiC nano-whisker addition on TiCN-based cements prepared by spark plasma sintering. *International Journal of Refractory Metals and Hard Materials, 34*, 36–40.
Ren, X., Peng, Z., Peng, Y., Fu, Z., Wang, C., Qi, L., & Miao, H. (2013). Effect of SiC nano-whisker addition on WC–Ni based cemented carbides fabricated by hot-press sintering. *International Journal of Refractory Metals and Hard Materials, 36*, 294–299.
Saulat, H., Cao, M., Khan, M. M., Khan, M., Khan, M. M., & Rehman, A. (2020). Preparation and applications of calcium carbonate whisker with a special focus on construction materials. *Construction and Building Materials, 236*, 117613.
Shi, T., Li, Z., Guo, J., Gong, H., & Gu, C. (2019). Research progress on CNTs/CNFs-modified cement-based composites—A review. *Construction and Building Materials, 202*, 290–307.
Silvestroni, L., Sciti, D., Melandri, C., & Guicciardi, S. (2010). Toughened ZrB2-based ceramics through SiC whisker or SiC chopped fiber additions. *Journal of the European Ceramic Society, 30*(11), 2155–2164.
Wang, C., Li, K.-Z., Li, H.-J., Jiao, G.-S., Lu, J., & Hou, D.-S. (2008). Effect of carbon fiber dispersion on the mechanical properties of carbon fiber-reinforced cement-based composites. *Materials Science and Engineering: A, 487*(1), 52–57.
Wang, C., Li, W., & Huang, M. (2019). High precision wide range online chemical oxygen demand measurement method based on ultraviolet absorption spectroscopy and full-spectrum data analysis. *Sensors and Actuators B: Chemical, 300*, 126943.
Xiong, K., Xu, G., Li, S., & Song, C. (2008). Dispersion stability of silicon carbon whisker. *Bulletin of the Chinese Ceramics Society, 36*(10), 1432–1436.
Yang, L., Xie, H., Fang, S., Huang, C., Yang, A., & Chao, Y. J. (2021). Experimental study on mechanical properties and damage mechanism of basalt fiber reinforced concrete under uniaxial compression. *Structures, 31*, 330–340.
Yao, J., Yang, Y., & Chen, J. (2020). A novel chemo-mechanical model for fracture toughness of mortar under sulfate attack. *Theoretical and Applied Fracture Mechanics, 109*, 102762.
Zhan, M., Pan, G., Zhou, F., Mi, R., & Shah. (2020). In situ-grown carbon nanotubes enhanced cement-based materials with multifunctionality. *Cement and Concrete Composites, 108*, 103518.
Zhang, C., Kong, X., & Lu, Z. (2018). Application of digital image correlation method in mechanical properties test of polymer modified mortar. *Bulletin of the Chinese Ceramics Society, 46*(2), 187–192.
Zhang, X. N., Geng, L., & Wang, G. S. (2006). Fabrication of Al-based hybrid composites reinforced with SiC whiskers and SiC nanoparticles by squeeze casting. *Journal of Materials Processing Technology, 176*(1), 146–151.
Zhang, X., Xu, L., Du, S., Han, W., Han, J., & Liu, C. (2008). Thermal shock behavior of SiC-whisker-reinforced diboride ultrahigh-temperature ceramics. *Scripta Materialia, 59*(1), 55–58.
Zhao, X., Yang, J., Xin, H., Wang, X., Zhang, L., He, F., Liu, Q., & Zhang, W. (2018). Improved dispersion of SiC whisker in nano hydroxyapatite and effect of atmospheres on sintering of the SiC whisker reinforced nano hydroxyapatite composites. *Materials Science and Engineering: C, 91*, 135–145.
Zhou, B., Zhang, M., Wang, L., & Ma, G. (2021). Experimental study on mechanical property and microstructure of cement mortar reinforced with elaborately recycled GFRP fiber. *Cement and Concrete Composites, 117*, 103908.
Zhu, H., Zhou, H., & Gou, H. (2021). Evaluation of carbon fiber dispersion in cement-based materials using mechanical properties, conductivity, mass variation coefficient, and microstructure. *Construction and Building Materials, 266*, 120891.

Publisher's Note